Baltimore, Maryland
NOISE-CON 2004
2004 July 12-14

Nonlinear Propagation of Noise Radiated from Supersonic Jets

Kent L. Gee
Benoit P. Petitjean
Dennis K. McLaughlin
Victor W. Sparrow
The Pennsylvania State University
University Park PA 16802

1. INTRODUCTION

The role of nonlinearity in the propagation of noise from supersonic jets is not currently well understood, but it is of interest because the noise radiation from military jet aircraft can approach or exceed levels of 150 dB re 20 μPa or more at close range[1]. These high noise amplitudes suggest that the inclusion of nonlinear propagation effects in long-range noise estimation models may be of importance in order to correctly assess the environmental impact the aircraft have.

A finite-amplitude noise spectrum undergoes an evolution as it propagates, in that energy is transferred from mid to higher frequencies, and in some cases, from mid to lower frequencies, resulting in a spectral broadening. Waveform steepening accounts for the energy transfer to high frequencies as portions of the waveform become more shock-like. If these steepened portions begin to coalesce, the number of zero crossings decreases, consequently resulting in an energy increase at lower frequencies. The nonlinear propagation of noise has been studied over the past few decades by, among many others, Rudenko and Soluyan[2], Gurbatov *et al.*[3], Blackstock and colleagues[4,5], Howell and Morfey[6,7], and Crighton and Bashforth[8,9]. While many of these studies employed a variety of theoretical and numerical techniques in an attempt to understand and predict the nonlinear spectral evolution, few have included accompanying experimental evidence. Crighton[9], in particular, has stressed the need for additional aeroacoustic experiments in order to properly assess the relevance and accuracy of the abundance of analytical and numerical work already carried out.

Recent laboratory experiments performed on both cold and heat-simulated (HS) model-scale supersonic jets demonstrate evidence of nonlinear propagation effects[10]. This paper represents continued analysis of those data. The experimental setup is first briefly described and is followed by the presentation of power spectral results. Nonlinearity indicators, based on work by Howell and Morfey, are discussed next. The current experimental data are then compared to two existing nonlinear spectral evolution methods developed by Howell and Morfey[6,7] and Crighton and Bashforth[8,9], followed by some conclusions and recommendations for further work in the area.

2. EXPERIMENTAL SETUP

The experiments described in this paper were carried out in the Pennsylvania State University high-speed jet noise facility[10], where a compressed air supply is passed through a jet plenum and nozzle into an anechoic chamber equipped with a highly muffled exhaust fan. For the cold jet, the static temperature ratio to that of ambient was 0.69. For the HS case, the simulated static temperature ratio inside the jet to ambient was 2.5. The heated jet properties are simulated using a helium/air mixture, which matches the speed of sound inside the jet, U_j, to that of the heated jet via a density rather than temperature change. A series of valves controls the flow of helium, which is injected into the flow upstream of the nozzle in order to allow for mixing of the gases prior to being exhausted into the measurement environment. The nozzle used for these tests was a 12.7 mm (0.5 in) converging-diverging circular nozzle designed for a flow of M_j = 1.5, where M_j signifies the jet Mach number. For M_j = 1.5 and temperature ratios of 2.5 and 0.69, the corresponding U_j is approximately 816 m/s for the HS jet and 429 m/s for the cold jet.

Acoustic pressure waveforms were recorded using a linear array of 3.175 mm (0.125 in) Bruel and Kjaer microphones at normal incidence and located at 15, 30, 60, and 100 D_j (jet diameters) along the 35° radial measured from the nozzle axis. The microphone locations were measured relative to an origin located 5 D_j from the end of the nozzle, which corresponds roughly to the end of the potential core.

Because 15 D_j is almost certainly in the acoustical near field of the jet, only data from the latter three measurement distances are considered in the analysis. Analog-to-digital conversion of the microphone data was carried out using a National Instruments high-speed data acquisition board sampling at approximately 298.5 kHz. The data were filtered using an 8-pole high pass filter with a cutoff frequency of 500 Hz and a 4-pole low pass anti-aliasing filter with a cutoff frequency of 120 kHz. Average power spectral densities (PSD) were processed by first dividing approximately 0.7 seconds of data into 1024-point blocks with 50 percent overlap and applying a Hanning window to each block. The mean PSD was then calculated from the average of the magnitude-squared discrete Fourier transform (DFT) for each block of data. Amplitude corrections for the microphone actuator and free-field responses were also applied to the PSD and other analyses.

3. RESULTS AND DISCUSSION

A. Spectral Measurements vs. Linear Extrapolations

In this section, measured PSD results are presented and analyzed. While jet noise spectra are often displayed using a Strouhal number scaling for frequency ($St = f * D_j / U_j$), this has not been done for this analysis in order to plot both the cold and HS spectra on the same axes. The frequency range considered, 500-100,000 Hz, corresponds to *St* ranges of 0.01-1.56 for the HS jet and 0.02-2.96 for the cold jet. Also a fairly standard practice with jet noise results is to remove the effects of ambient conditions on propagation by correcting spectra for atmospheric absorption. These are referred to as lossless spectra. A correction based on the absorption model developed by Bass *et al*.[11,12] has been applied to the PSD results that follow.

In Fig. 1, the measured PSD at 100 D_j for the HS and cold jets along with linear extrapolations from 30 and 60 D_j. Because the spectra are lossless, the linear extrapolation is simply the application of spherical spreading, which causes a reduction in level of 10.5 dB between 30 and 100 D_j and 4.4 dB between 60 and 100 D_j. For the HS case, the measured overall sound pressure levels (OASPL) at the three distances were 142.6, 135.0, and 130.0 dB re 20 μPa. The measured OASPL for the cold jet were 129.8, 124.4, and 120.0 dB re 20 μPa. The OASPL was calculated by summing up the PSD over all frequency bins, multiplying by the bin width, and converting to dB re 20 μPa. The noise radiated from the cold jet shows little evidence of nonlinear propagation in that from approximately 8-70 kHz, the two extrapolations collapse very well with the 100 D_j measurement. The small discrepancy above 70 kHz is believed to be due to errors in the 60 and 100 D_j microphone free-field corrections. Below 8 kHz, the 60 D_j extrapolation collapses fairly well with the 100 D_j measurement, whereas the 30 D_j extrapolation does not. This phenomenon may perhaps be explained in terms of a discussion of the geometric far field (GFF) for jet noise.

A recent study carried out by Koch *et al.*[13] on the location of the GFF for subsonic (M_j = 0.5, 0.9) cold jets resulted in a determination that the beginning of the GFF, where an assumption of spherical spreading is valid, is frequency-dependent. The high-frequency noise generation process occurs fairly close to the end of the jet and its GFF is consequently reached earlier than low-frequency noise, the source of which appears to be more extended in nature. Their analysis resulted in a determination that the GFF for all frequencies of interest has been reached by approximately 50 D_j. While a parallel investigation has not been carried out for the noise radiated from supersonic jets, the frequency-dependent nature of the GFF will continue to be true. The behavior of the cold jet spectral data in Fig. 1 can be plausibly explained in terms of the frequency-dependent GFF. For frequencies below 8 kHz, 30 D_j corresponds to the near field where non-spherical geometric spreading occurs, whereas by 60 D_j the GFF has been reached for all frequencies. While this interpretation simply places the GFF between 30 and 60 D_j for this supersonic cold jet, it is consistent with the conclusions of Koch *et al*. made for subsonic cold jets.

The HS jet spectra in Fig. 1 exhibit different trends from those of the cold jet in that there appears to be a relative loss of energy from mid-frequencies and the high-frequency slope is increasing as a function of distance, although more so between 30 and 60 D_j than 60 and 100 D_j. Above 70 kHz, even though the spectral levels are in error due to the microphone correction issues, comparison with the cold jet spectral discrepancies show that the slope changes would continue out to 100 kHz. It must be stated that how the location of the GFF changes between the cold and HS jet is not precisely known, however, the consistency in slopes between the two 30 D_j spectra suggests that the spatial extent of the cold and HS aeroacoustic sources is similar and that the location of the GFF would also be similar. This is a fairly important point to consider because the apparent shift of energy to lower frequencies evidenced by the change in peak frequency between 30 and 60 D_j could either be due to shock coalescence or simply non-

spherical spreading due to the extent of the near field. The fact that the HS measured level is below the extrapolated level, contrasted with the cold jet spectra, certainly implies that nonlinear energy loss is occurring at those frequencies; however, based on the cold jet GFF analysis, the shift in spectral peak is likely to be least partially due to near-field effects.

B. Howell-Morfey Indicators of Nonlinearity

The spectral results shown in the previous section demonstrate little change in the cold jet spectrum as a function of range but more appreciable spectral evolution for the case of the HS jet. A nonlinearity indicator based on the work of Howell and Morfey may be used to strengthen the assertion that the HS jet spectral changes are due to nonlinear propagation effects.

Howell and Morfey published a series of papers (see Ref. 7) on the development of a nonlinear prediction method suitable for long-range jet noise propagation. One of the model equations derived, while not suitable for prediction purposes, proved to be useful in the development of a nonlinearity indicator. This equation (essentially Eq. 5 in Ref. 6) may be written as

$$\frac{\partial}{\partial r}\left[r^2 e^{2\alpha(\omega)r} S_p(\omega, r)\right] = -\omega\left(\frac{\beta}{\rho_0 c_0}\right) r^2 e^{2\alpha(\omega)r} Q_{p^2p}(\omega, r), \tag{1}$$

where r, ω, α, and β are range, radian frequency, absorption coefficient, and coefficient of nonlinearity. S_p is the PSD and Q_{p^2p} is the imaginary part of the cross-spectral density calculated between $p^2(t)$ and $p(t)$, written as

$$Q_{p^2p}(\omega) = \mathrm{Im}\left(\Im\left\{p^2(t)\right\}\Im^*\left\{p(t)\right\}\right). \tag{2}$$

The symbols $\Im$ and * in Eq. 2 respectively represent Fourier transform and complex conjugation operators. In short, the left-hand side of Eq. 1 contains the derivative with respect to range of the PSD corrected for absorption and spherical spreading. If the propagation were purely linear, this would be a homogeneous ordinary differential equation for all r, which means that any nonlinear spectral distortion must be a consequence of a nonzero Q_{p^2p} calculation. If Q_{p^2p} is negative for a given frequency in Eq. 1, it means that the energy content at that frequency is increasing because of nonlinear interaction; if Q_{p^2p} is positive, energy is being transferred to other frequencies. In Ref. 6, the authors suggest an appropriate nonlinearity indicator to be a nondimensionalized version of Q_{p^2p}, dubbed *Q/S*, which is calculated by dividing Q_{p^2p} by S_p multiplied by the root-mean-square pressure. Calculations of *Q/S* for F/A-18E/F data were published in Ref. 1, where *Q/S* was essentially zero for the idle engine condition, but nonzero for military thrust and afterburner settings.

In Fig. 2, *Q/S* is shown at 30 D_j for both the cold and HS cases. Because the random errors associated with Q_{p^2p} appear to be greater than for the PSD due the fact that phase information is kept, the number of samples used in each DFT has been reduced to 512 to allow for a greater number of averages. The results in Fig. 2 show similar results for both the cold and HS jets in that there is a frequency range between about 6 and 20 kHz where *Q/S* is positive, meaning that energy is being lost to other frequencies where *Q/S* is negative, namely below 6 kHz and above 20 kHz. The estimate for the cold jet is noisier than for the HS case, presumably because *Q/S* is calculated by dividing two relatively small quantities, resulting in more variability. Also, as frequency increases 100 kHz, *Q/S* begins to lessen; however, it is likely that the estimate of Q_{p^2p} is in error at these high frequencies because the microphone free-field correction for phase is unknown.

The fact that *Q/S* is approximately equal for both the cold and HS jets leads to some question as to the utility of the nondimensionalization of Q_{p^2p}. Because the OASPL for the two cases differ by over 12 dB at 30 *Dj*, the amount of nonlinearity expected for the two cases should be very different. While *Q/S* is useful in determining the frequency ranges for which nonlinear energy transfer is positive or negative, it apparently gives no indication of the magnitude of the energy transfer. For that reason, it was decided to fully evaluate the right-hand side of Eq. 1, which not only yields the frequency regions of energy transfer,

but also the magnitude of the rate of energy transfer as a function of frequency. Because of the minus sign in Eq. 1, the result has exactly the opposite interpretation as described for Q_{p^2p}. Figures 3 and 4 display the results of that evaluation at 30 D_j and 100 D_j. A comparison between the cold and HS results for both distances reveals that the nonlinearity in the HS case is much greater. Although in Fig. 3 there is a region below 7 kHz that suggests a nonlinear transfer of energy to lower frequencies, it must be pointed out that Eq. 1 is only strictly valid in the GFF because of the assumption of spherical spreading. It is uncertain how much shock coalescence is actually taking place at 30 D_j because the lower frequency region for which Q_{p^2p} is negative is likely to still be in the near field. Furthermore, at 100 D_j, where the GFF is more likely to have been reached, the same frequency range appears to be losing energy. As a final point of analysis regarding the results in Figs. 3 and 4, it should be noted that the rate of energy transfer decreases by an order of magnitude between 30 and 100 D_j, suggesting that the nonlinear evolution slows as range increases, which it appears to happen when the HS jet PSD results at 30, 60, and 100 D_j in Fig. 1 are compared.

4. PREDICTION METHODS COMPARISON

As a final analysis, the 100 D_j data are compared against two nonlinear propagation algorithms using the 30 D_j spectra as inputs. Long-range nonlinear spectral evolution models for high-amplitude jet noise were proposed in the early 1980's, by Crighton and Bashforth[8,9] (CB) and Howell and Morfey[6,7] (HM). Because the CB and HM methods are well developed in their original references, their main details are simply summarized below. The CB method is a series expansion solution for the power spectrum, which has its roots in an ensemble-averaged version of the Burgers equation, the simplest nonlinear wave equation that includes the effects of nonlinearity and losses. In the CB model, spherical spreading and arbitrary atmospheric absorption are included, and a Gaussian source assumption is made. Because the series solution is truncated after second order, it suffers from range limitations that are both amplitude and frequency dependent. However, the method was intended to be valid for several hundred jet diameters, which is much greater than the range considered here.

The HM method also begins with a series expansion solution of the Burgers equation for the power spectrum; however, it differs from the CB method in that individual terms of the Taylor series, which consist of derivatives of the power spectrum with respect to range, are equated with terms involving higher order spectra, which result from analytically evaluating the derivatives. The outcome is a potentially infinite set of ordinary differential equations that can be each used to describe the evolution of the power spectrum as function of range. Equation 1 is the first order equation in that set. However, the difficulty with using Eq. 1 as a model equation is that Q_{p^2p} will vary in an unknown fashion along the propagation path. This same difficulty arises with each of the prediction equations involving higher order derivatives and the problem remains insoluble unless the higher order spectra can be rewritten solely in terms of the PSD at all range points. To do this, the HM method employs a quasi-normal propagation assumption, which requires that all higher order spectra remain related to the PSD in a Gaussian fashion. This in turn means that all odd-order spectra are considered negligible and that even-order spectra can be calculated from the power spectrum. Because the quasi-normal hypothesis forces Eq. 1 to be homogeneous, resulting in no spectral distortion, a different model equation must be sought. The equation used for prediction of the power spectral evolution results from the second-order term in the series expansion. As is the case with the CB method, a Gaussian source assumption is used at the input.

These methods have been compared against F/A-18E/F data in Ref. 1, yielding little agreement between the data and the prediction results. The motivation for making additional comparisons against the model-scale jet data is the fact that the amplitude of the HS jet is approximately 8-9 dB less than the full-scale afterburner measurement at comparable distances may cause the two methods to compare more favorably with the measured spectra. The results from propagating the 30 D_j cold and HS spectra out to 100 D_j using the CB and HM algorithms are shown in Fig. 5, along with the measured spectra at 100 D_j and the linear extrapolation from 30 D_j. The first conclusion that can be made is that for both cases, the prediction methods converge to the linear solution as frequency decreases. Neither method predicts any shift of energy to lower frequencies, although the extent to which they should is unknown at this point, due to the near/far field question already raised. The prediction results for the cold jet only differ very slightly (less than 1 dB) from the linear prediction at high frequencies and are therefore consistent with the 100 D_j measurement.

The HM and CB results for the HS jet in Fig. 5 differ substantially from the linear prediction at high frequencies, and to a lesser extent, from each other. In order to more easily compare the results, the apparent nonlinear gain (ANG) is plotted as a function of frequency in Fig. 6. The ANG in Fig. 6 is calculated by normalizing each of the results at 100 D_j by the linear extrapolation from 30 D_j and plotting it on a dB scale. It is the "apparent" nonlinear gain because the near-field effects or microphone response correction errors previously discussed are included in the ANG and could potentially be interpreted as being due to nonlinearity. A number of statements may be made about the comparison between the CB and HM predictions and the 100 D_j HS measurement. The first is that although both methods predict a small amount of energy loss in the 5-15 kHz region where the ANG is negative, the actual measured energy loss is much greater. On a positive note, however, there is rough agreement between the ANG slopes of the CB and HM results and the measured spectrum between 10 and 70 kHz, at which point the ANG for the measured spectrum suddenly decreases due to the microphone free-field correction issues. Finally, similar comparisons have been made from 60 D_j; however, the high-frequency correction errors present in the input spectrum at this distance make the comparison less meaningful, especially for the HS case.

5. CONCLUSIONS

An analysis of the nonlinear propagation of noise emitted from model-scale jets from 30 to 100 D_j has been described. No nonlinear spectral distortion is evident in the cold jet spectra; however, a transfer of energy occurs from mid to high frequencies in the HS jet spectra. There is also an apparent shift of energy to lower frequencies, particularly between 30 and 60 D_j, but evidence based on the cold jet results suggests that this phenomenon could be linked to near-field effects (e.g., non-spherical geometric spreading) rather than shock coalescence. A comparison between linear extrapolations from 30 and 60 D_j and the 100 D_j PSD measurement for the cold jet implies that the frequency-independent GFF begins somewhere between 30 and 60 D_j for these source conditions and this angle.

Calculations of a nonlinearity indicator, Q/S, proposed by Howell and Morfey have been carried out and discussed. While this indicator appears to be useful in determining the regions of positive and negative energy transfer, it fails to give any indication of the amount of nonlinearity occurring at a given location because of the normalization chosen. A more appropriate indicator, also based on the work of Howell and Morfey but which does not contain the normalization, has been calculated and is more successful in showing not only the gain/loss of energy at a given location and frequency, but the magnitude of the energy transfer rate as well.

Comparisons between the experimental data and two nonlinear spectral prediction methods have also been carried out. Both the CB and HM methods predict virtually no nonlinearity in the case of the cold jet; however, for the HS jet, they predict slightly different amounts energy transfer to high frequencies. While the amount of nonlinear gain as function of frequency agrees with the slope of that of the actual measurement over a broad frequency range, neither method predicts the amount of loss that actually occurs in the peak frequency region. While the disparity between measurement and prediction is less than in Ref. 1 for the full-scale comparisons, the measurement range is also less. The results of this comparison corroborate the conclusion made from the previous investigation, that a simple nonlinearity prediction algorithm that operates solely on the power spectrum appears implausible. When the phase information is neglected, so is a large portion of the actual physics of the propagation, because different waveforms with the same power spectra may undergo different amounts of nonlinear distortion as they propagate[4].

Finally, some issues raised by the results of this study merit brief mention. First of all, while the current results demonstrate the ability to generate jet noise with nonlinear propagation characteristics, future work should involve the use of nozzles with larger diameters. The reason for this is two-fold. First, since the peak frequency of the PSD scales as the inverse of the diameter, an increase in nozzle diameter would shift the spectrum down in frequency, thus lessening the importance of errors in microphone response corrections at high frequencies. Second, the current HS data at 100 kHz scales to a St = 1.56. For a military jet aircraft with a nozzle diameter of 0.6 m and equivalent M_j and U_j, St = 1.56 is equivalent to a frequency of approximately 2.1 kHz. Because it is likely that an appreciable amount of energy is transferred to frequencies corresponding to St > 1.56 (frequencies important in determining perceived noise levels[9]), the use of a larger nozzle would extend the observable frequency range, where the disparity between linear predictions and measurements should be greater. Such measurements, coupled with the development of more physically-based finite-amplitude noise propagation models, will help more fully determine the role of nonlinearity in the radiation of noise from supersonic jets.

6. ACKNOWLEDGMENTS

The authors are supported by a grant from the Strategic Environmental Research and Development Program through a subcontract by Wyle Laboratories, monitored by Dr. Kenneth Plotkin and Dr. Micah Downing. The authors are also grateful to Dr. Philip Morris for several helpful insights related to this analysis.

References

1. K. L. Gee, T. B. Gabrielson, A. A. Atchley, and V. W. Sparrow, "Preliminary analysis of nonlinearity in F/A-18E/F noise propagation," AIAA Paper no. 2004-3009, 10th AIAA/CEAS Aeroacoustics Conference, Manchester, England, 2004.
2. O. V. Rudenko and S. I. Soluyan, *Theoretical Foundations of Nonlinear Acoustics*, (Plenum, New York, 1977), Chapter 10.
3. S. N. Gurbatov, A. N. Malakhov, and A. I. Saichev, *Nonlinear Random Waves and Turbulence in Nondispersive Media: Waves, Rays, and Particles* (Manchester Univ. Press, Manchester, 1991).
4. D. A. Webster and D. T. Blackstock, "Experimental investigation of outdoor propagation of finite-amplitude noise," NASA Contractor Report 2992, 1978
5. F. M. Pestorius and D. T. Blackstock, "Propagation of finite-amplitude noise," in *Finite-amplitude Wave Effects in Fluids,* Proc 1973 Symposium, Copenhagen, edited by L. Bjørnø (IPC Science and Technology Press, Ltd., Guildford, England, 1974), pp. 24-29.
6. C. L. Morfey and G. P. Howell, "Nonlinear propagation of aircraft noise in the atmosphere," AIAA J., **19**, pp. 986-992 (1981).
7. G. P. Howell and C. L. Morfey, "Non-linear propagation of broadband noise signals," J. Sound Vib., **114**, pp. 189-201 (1987).
8. D. G. Crighton and S. Bashforth, "Nonlinear propagation of broadband jet noise," AIAA Paper no. 80-1039, AIAA 6th Aeroacoustics Conf., Hartford, Connecticut, 1980.
9. D. G. Crighton, "Nonlinear acoustic propagation of broadband noise," in *Recent Advances in Aeroacoustics,* Proc 1983 International Symposium on Recent Advances in Aerodynamics and Acoustics, edited by A. Krothapalli and C. A. Smith (Springer & Verlag, New York, 1984), pp. 411-454.
10. B. P. Petitjean and D. K. McLaughlin, "Experiments on the nonlinear propagation of noise from supersonic jets," AIAA Paper no. 2003-3127, 9th AIAA/CEAS Aeroacoustics Conf., Hilton Head, South Carolina, 2003.
11. H. E. Bass, L. C. Sutherland, A. J. Zuckerwar, D. T Blackstock, and D. M. Hester, "Atmospheric absorption of sound: Further developments," J. Acoust. Soc. Am., **97**, pp. 680-683 (1995).
12. H. E. Bass, L. C. Sutherland, A. J. Zuckerwar, D. T Blackstock, and D. M. Hester, "Erratum: Atmospheric absorption of sound: Further developments," J. Acoust. Soc. Am., **99**, p. 1259 (1996).
13. L. D. Koch, J. Bridges, C. Brown, and A. Khavaran, "Numerical and experimental determination of the geometric far field for round jets," NASA Technical Memorandum 2003-212379.

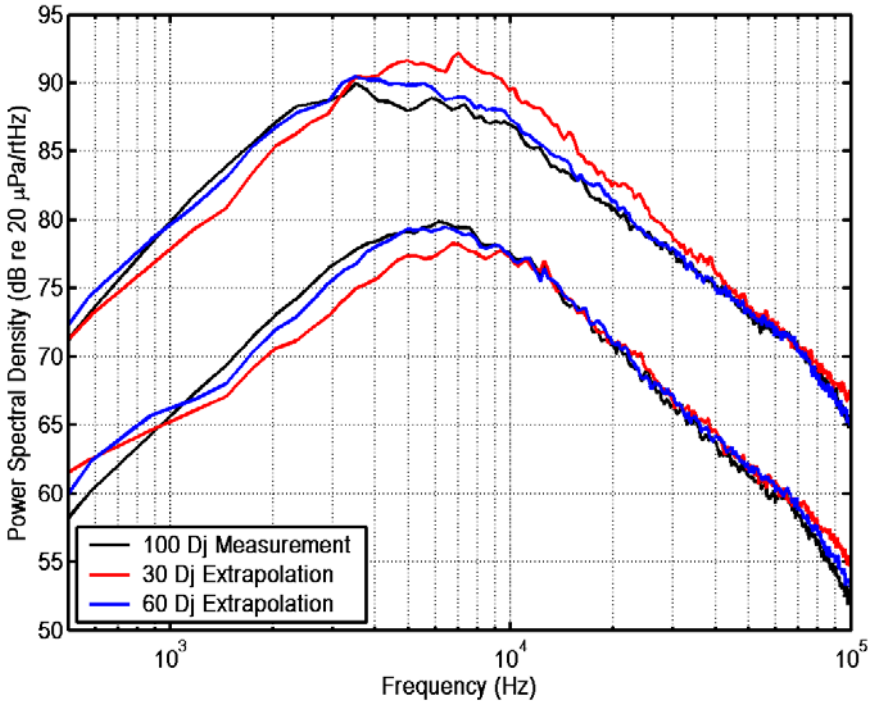

Figure 1. Measured and linearly extrapolated lossless PSD at 100 D_j, for the heat-simulated jet (upper set of curves) and the cold jet (lower set of curves).

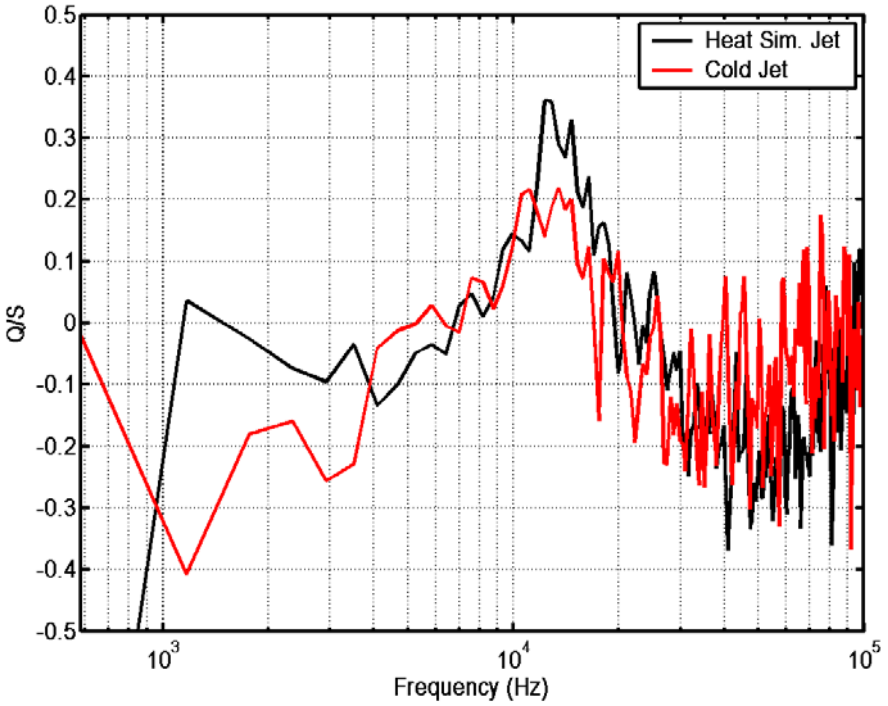

Figure 2. The Howell-Morfey nonlinearity indicator, *Q/S*, calculated at 30 D_j.

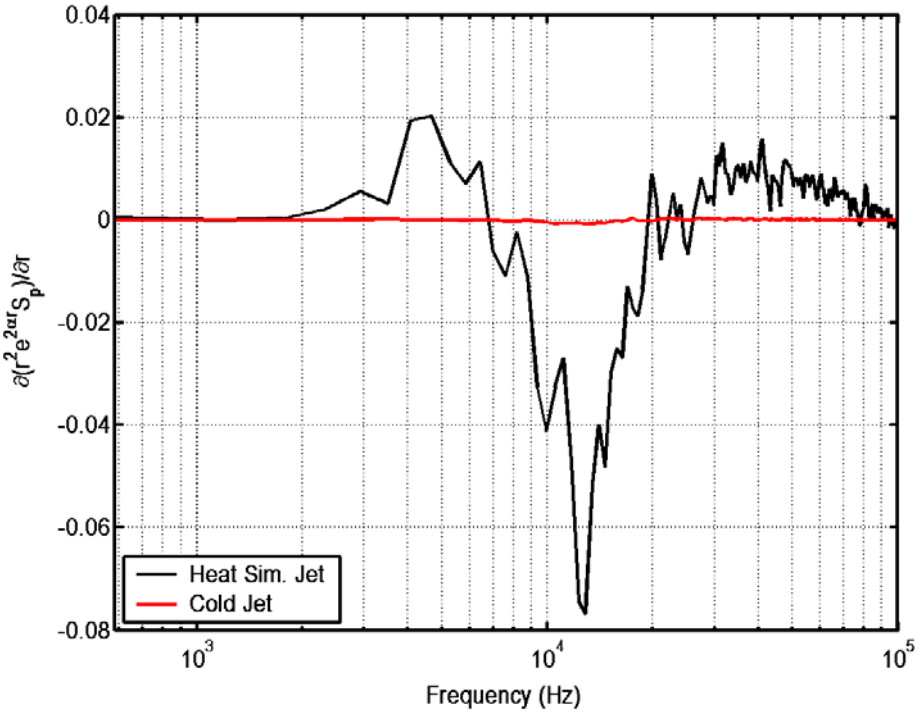

Figure 3. The right-hand side of Eq. 1 evaluated at 30 D_j as an indicator of the nonlinear transfer of energy between frequencies.

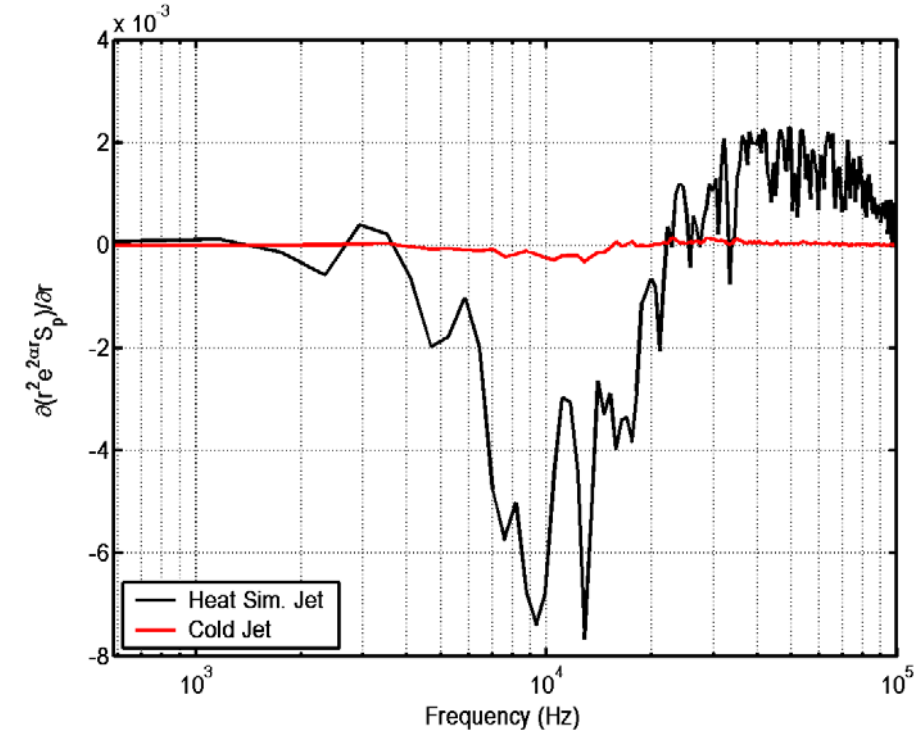

Figure 4. The right-hand side of Eq. 1 evaluated at 100 D_j as an indicator of the nonlinear transfer of energy between frequencies.

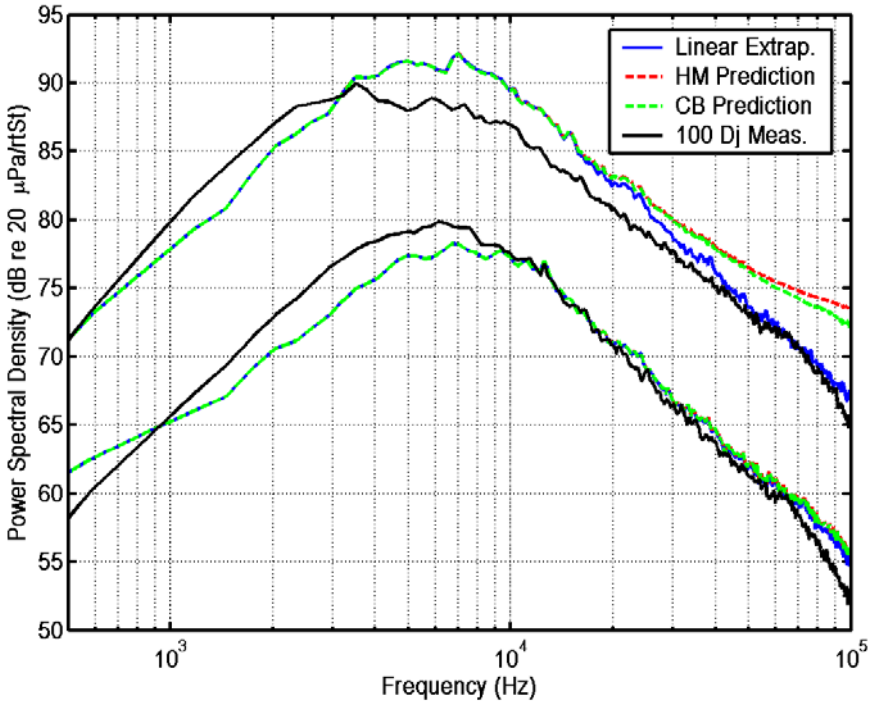

Figure 5. Linear, HM, and CB prediction results propagated out to 100 D_j from 30 D_j. Comparisons are made with the lossless measured PSD for the HS jet (upper curves) and the cold jet (lower curves).

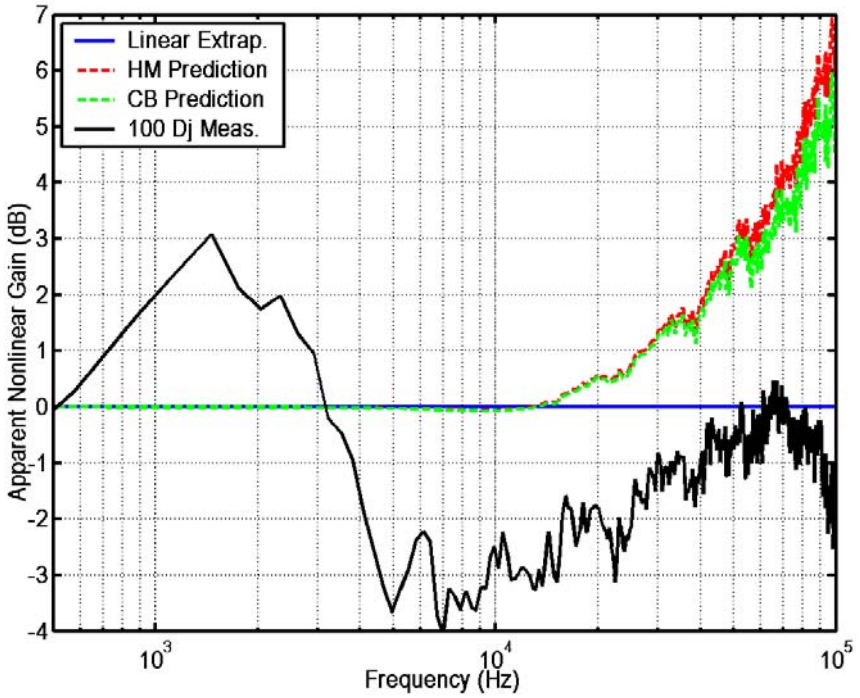

Figure 6. Apparent Nonlinear Gain calculated for the HS jet results in Fig. 5.